Topology-Guided Cyclic Brain Connectivity Generation using Geometric Deep Learning

Sserwadda, Abubakhari; Rekik, Islem

Published in:
Journal of Neuroscience Methods

DOI:
10.1016/j.jneumeth.2020.108988

Publication date:
2021

Topology-Guided Cyclic Brain Connectivity Generation using Geometric Deep Learning

Abubakhari Sserwadda, Islem Rekik

PII: S0165-0270(20)30411-8

DOI: https://doi.org/10.1016/j.jneumeth.2020.108988

Reference: NSM 108988

To appear in: *Journal of Neuroscience Methods*

Received Date: 15 July 2020

Revised Date: 23 September 2020

Accepted Date: 20 October 2020

Please cite this article as: Abubakhari Sserwadda, Islem Rekik, Topology-Guided Cyclic Brain Connectivity Generation using Geometric Deep Learning, *<![CDATA[Journal of Neuroscience Methods]]>* (2020), doi: https://doi.org/

Topology-Guided Cyclic Brain Connectivity Generation using Geometric Deep Learning

Abubakhari Sserwadda[a], Islem Rekik[a,b,*]

[a] *BASIRA lab, Faculty of Computer and Informatics, Istanbul Technical University, Istanbul, Turkey*
[b] *School of Science and Engineering, Computing, University of Dundee, UK*

Abstract

-Background. There is a growing need for analyzing medical data such as brain connectomes. However, the unavailability of large-scale training samples increases risks of model over-fitting. Recently, deep learning (DL) architectures quickly gained momentum in synthesizing medical data. However, such frameworks are primarily designed for Euclidean data (eg., images), overlooking geometric data (eg., brain connectomes). A few existing geometric DL works that aimed to predict a target brain connectome from a source one primarily focused on domain alignment and were agnostic to preserving the connectome topology.

-New Method. To address the above limitations, firstly, we adapt the graph translation generative adversarial network (GT GAN) architecture to brain connectomic data. Secondly, we extend the baseline GT GAN to a *cyclic* graph translation (CGT) GAN, allowing bidirectional brain network translation between the source and target views. Finally, to preserve the topological strength of brain regions of interest (ROIs), we impose a topological strength constraint on the CGT GAN learning, thereby introducing CGTS GAN architecture.

-Comparison with existing methods. We compared CGTS with graph translation methods and its ablated versions.

-Results. Our deep graph network outperformed the baseline comparison method and its ablated versions in mean squared error (MSE) using multiview autism spectrum disorder connectomic dataset.

*Corresponding author; Dr Islem Rekik, http://basira-lab.com/, CGTS GAN code is available at: https://github.com/basiralab/CGTS-GAN

-Conclusion. We designed a topology-aware bidirectional brain connectome synthesis framework rooted in geometric deep learning, which can be used for data augmentation in clinical diagnosis.

Keywords: Brain connectome generation, geometric deep learning, cyclic adversarial graph translation, topological strength

1. Introduction

Brain connectivities established by synapses reveal the statistical interactions or information flow among distinct anatomical brain regions of interest (ROIs) within the nervous system (Bullmore and Sporns, 2009; Bassett and Sporns, 2017). The strength of brain connectivity influences the neural activities in the brain as it determines which brain regions are strongly or weakly connected physically or functionally. Brain connectivity measures are biomarkers of neural disorders such as Alzheimer's disease (delEtoile and Adeli, 2017) and Autism Spectrum Disorder (ASD) (Jeste et al., 2015) which is a neurodevelopmental disorder that is characterised by deficits in social skills, speech, and behavior. Hence, understanding how such disorders disconnect the brain wiring or cause atypical alterations is fundamental in revealing the mechanism with which these kick off and develop. The field of network neuroscience (Bassett and Sporns, 2017), where graph theory meets brain connectivity, presented a compact representation of the human brain connectome derived from non-invasive magnetic resonance imaging (MRI) of the brain. Specifically, the brain is modelled as a network composed of nodes (brain ROI) and edges as connections between nodes and by so doing, interactions between every possible brain anatomical regions is established (de Vico Fallani et al., 2014; Soares et al., 2016; Mahjoub et al., 2018; Lisowska et al., 2018). This graphical modelling of the whole-brain network enables the usage of graph theory metrics to study important topological properties of brain connectome like centrality, clustering-coefficient, characteristic path length, modularity and information flow efficiencies (e.g, global and diffusion efficiency) for analyzing connectional patterns in brain connectomes. In general, these properties give insights into functional integration, segregation, resilience or organization of the brain network as whole or the individual brain ROI in both healthy and disordered populations (Bullmore and Bassett, 2011; Reijneveld et al., 2007; Damoiseaux et al., 2006).

Brain connectomic acquisition has been enhanced by the evolution of various structural MRI modalities including T1-weighted imaging, resting-state functional MRI magnetisation transfer imaging, and diffusion-weighted imaging. Such diverse multimodal connectomic datasets are very vital in exploring the differences in anatomical ROIs connectivity patterns between healthy and disordered brains, among other purposes (Hinrichs et al., 2011; Zhang et al., 2011; Yuan et al., 2012; Tong et al., 2015; Farrell et al., 2009). The brain connectivity can be encoded in a single view representation or in multiple views where each view captures a particular relationship (e.g., functional or morphological) between pairs of brain ROIs; thus, offering additional significant information about the brain construct. Several promising research in network neuroscience has been conducted using multiview brain connectomes (Mahjoub et al., 2018; Lisowska et al., 2017; Raeper et al., 2018; Dhifallah et al., 2020, 2019a). In (Lisowska et al., 2017; Raeper et al., 2018) multiview brain networks were used for early dementia diagnosis, and in (Mahjoub et al., 2018) to discriminate between late mild cognitive impairment and Alzheimer's disease patients. In all these works, mutiview brain networks boosted the diagnostic power of learning models in comparison to using single view networks. (Dhifallah et al., 2020, 2019a) proposed machine learning based frameworks to learn how to integrate a population of multiview brain networks to estimate a holistic connectional brain template.

However, high costs of clinical diagnosis, medical technological challenges, among other reasons, renders the completion of all medical scans for all patients hard, leading to missing data samples, or brain views. For a number of existing connectomic studies, patients with missing data are generally discarded; yet, training predictive learning models on a few samples poses risks of model overfitting. To fill this gap, generative learning models and data completion frameworks have been designed to predict the missing samples. For instance, in (Wang et al., 2016) a semisupervised tripled dictionary learning-based method for predicting standard-dose PET (S-PET) image using low-dose PET (L-PET) and corresponding MRI is proposed. They used patch-based sparse representation on training dataset with a complete set of MRI, L-PET and S-PET modalities to construct the dictionary. Their proposed method is able to utilize samples with and without complete modalities, thus, improving the prediction peformance through efficient use of all the available training samples. Another study, in (Huang et al., 2016) proposed a nonlinear supervised sparse regression-based random forest (RF) framework for predicting several longitudinal AD clinical scores. Different from studies

that oftenly discarded subjects with missing scores, their proposed method first estimates those missing scores with a sparse regressionbased RF, and thereafter utilizes those estimated longitudinal scores for all the previous time points to predict the scores at the next time point. A detailed review of generative adversarial network in medical imaging is presented in (Yi et al., 2019).

However, these existing methods are mainly designed for Euclidean data (e.g., images) but not geometric data (e.g., brain connectomes). A very limited research has been made on synthesizing brain networks in particular. In (Zhu and Rekik, 2018), the first work on brain network prediction was presented based a novel sample selection strategy through canonical correlation analysis with multi-kernel connectomic manifold learning to predict multiview brain networks from a source view. However, this prediction was based on simple statistical tools and independent data processing blocks including domain alignment, sample selection and ultimately prediction. This somehow solves the problem in a dichotomized manner that does not allow the different learning blocks to improve their learning via feedback and information sharing.

On the other hand, researchers have embarked on geometrical deep learning (Levie et al., 2018) to tackle challenges associated with graphs and manifolds. Unlike popular fields like computer vision where image data is defined on Euclidean domains, graph data is non-Euclidean (ie. the shortest distance between two points is not necessarily a straight line). Such non-Euclidean data might have self-intersections, infinite curvature, different dimensions depending on the view scale and location and extreme variations in density. Thus, Euclidean geometric properties and Euclidian space representation including images where x and y coordinates represent pixel location and z for color/intensity may not directly hold for non-Euclidean data. In addition, vital basic computation operations such as convolution operations that are thoroughly explored in the Euclidean domains including images where a convolutional neural network (CNN) can sufficiently extract all patterns in image data, are not well defined on non-Euclidean spaces (Bronstein et al., 2017). In particular, a graph might have a varying size of unordered nodes, with nodes having varying size of neighbors and each node having links with other distant individual nodes. Such complexities render the deployment of spatially localized data operations including convolution and pooling on graph data non-obvious. Recent review papers (Wu et al., 2020; Zhou et al., 2018) have investigated approaches for extending deep learning on non-Euclidean

domains. Generative Adversarial Networks (GANs) (Goodfellow, 2016) and their extensions have been widely deployed to synthesize datasets with high levels of realism (Kazeminia et al., 2018; Armanious et al., 2020; Yi et al., 2019; Wu et al., 2018; Mahapatra et al., 2017). Recently, a few research works using GANs for graph-based data embedding and generation have been explored. In (Guo et al., 2018), a novel graph translation GAN was proposed as an extension of the conventional graph convolutional network (GCN) (Kipf and Welling, 2016) in addition to designing new graph deconvolution layers. Unlike graph generation methods that only aim at learning the graph distributions, this graph translation architecture simultaneously learns both the latent graph representation and generic translation mapping from the input graph to the target one. The GT GAN outperformed several existing state-of-the-art graph generation architectures including graph generation method based on sequential generation with LSTM model (You et al., 2018), GraphVAE which is a probability-based graph generation method for small graphs using variational autoencoders (Simonovsky and Komodakis, 2018), a graph neural networks based general approach for learning generative models over arbitrary graphs (Li et al., 2018), and RandomVAE which is a deep generative model for molecular graphs (Samanta et al., 2019). The GT GAN exhibited high ability to learn graph translation rules thereby significantly outperforming these comparison graph generation methods in both effectiveness and scalability; however, GT GAN architecture is unidirectional, (i.e., only caters for translation from source to a target graph at a time but not vice versa). Besides, it does not provide a special mechanism or constraint for conserving a distinct graph node topological pattern during the translation learning.

The first application of geometric deep learning in predicting brain networks in particular is presented in (Bessadok et al., 2019b). This work deploys an adversarial regularized graph convolutional autoencoder inspired by (Pan et al., 2018) to align the source and the target brain graph populations. The pipeline extracts features in both the source and target domains, and aligns domains symmetrically prior to the prediction step. Another related work (Bessadok et al., 2019a) also build on the same adversarial regularized graph convolution autoencoder (Pan et al., 2018) to learn hierarchical embeddings for aligning source and target domains in a coarse to fine manner. Although pioneering, in both works, the prediction step is independent from other data processing steps including alignment, thus a potential risk of error accumulation in the entire framework due to errors at each individual step of

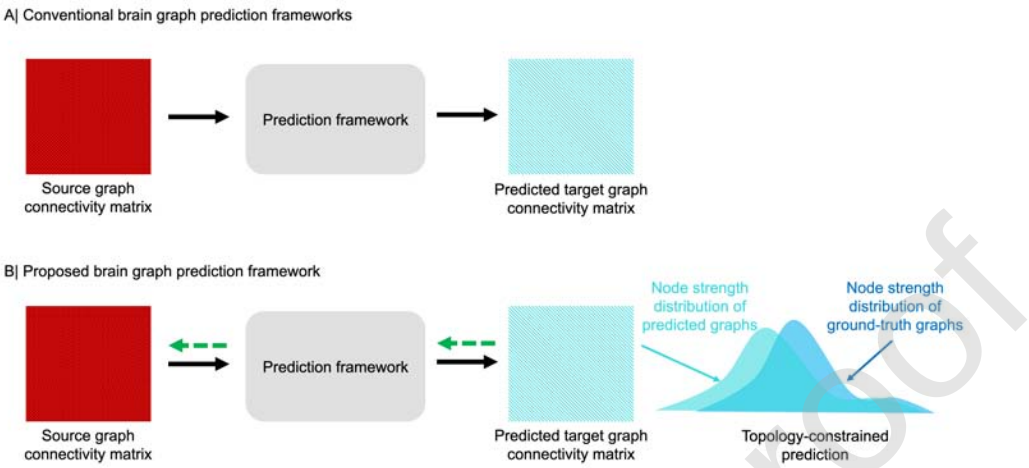

Figure 1: *Comparison between existing brain graph generation methods and our proposed method.* In comparison with existing learning-based frameworks for target brain graph prediction from a source graph, our proposed framework improves the source-to-target generation by (i) integrating a reverse prediction task from target to source graphs (dashed green arrows) and (ii) aligning the distribution of the node strength of the predicted target brain graphs with that of the ground-truth ones.

the pipeline. Besides, the prediction from source to target is unidirectional, which makes it prone to mode collapse in GANs (Zhu et al., 2017). Also, graph topological patterns are not necessarily preserved during the alignment and prediction steps (**Fig.** 1).

On the other hand, a cycle generative adversarial network (CGAN) proposed in (Zhu et al., 2017) adds cycle losses on top of the generative adversarial losses and allows bidirectional translation from the source to the target domain and solves the issue of GAN mode collapse. Another work (Zhou et al., 2019) applied cycle consistency in graph transfer mappings between domains so as to have sufficient similarity between the transferred and the target domains. However, this cyclic graph generation architecture may not preserve distinct topological properties of the brain network like the ROI strength, yet, it is so vital for synthesizing realistic brain connectomes. To address all these limitations, we propose CGTS: a Cyclic Graph Translation with topological Strength constraint to enforce the conservation of the brain ROI (i.e., node) topological strength of the generated brain graph in comparison to the ground truth target graph. We list below the main contributions

of our proposed CGTS brain connectome generation network (**Fig. 1**):

- First, we extend deep graph translation approach suggested in (Guo et al., 2018) to multiview brain connectomes.
- Second, to enforce a bidirectional network translation between the source and target domains while ensuring significant similarity between the predicted and target ground truth views, we propose a cyclic graph translation architecture, composed of a cycle loss, with an intuition that if we translate from the source view to the target view and back again, we should be able to we should obtain the source view we initially started with.
- Lastly, to generate a topologically sound target brain connectomes, we integrate a topological strength constraint into the brain network translation model.

2. Proposed method

In this section we detail the steps for the proposed brain graph generation architectures from a source graph. We denote matrices by boldface capital letters, e.g., $\mathbf{X}$, vectors are denoted by boldface lowercase letters, e.g., $\mathbf{x}$, and scalars are denoted by lowercase letters, e.g., x. For easy reference, we have summarized the major mathematical notations used in this paper in Table 1.

Table 1: *Key mathematical notations used in this paper.*

Mathematical notation	Definition
N	total number of subjects in the population
n_r	total number of regions of interest in the brain (ROIs)
$\mathbf{X}_i$	source graph view for the i^{th} subject $\in \mathbb{R}^{n_r \times n_r}$
$\mathbf{Y}_i$	target graph view for the i^{th} subject $\in \mathbb{R}^{n_r \times n_r}$
$\mathbf{W}_{ij}$	weighted adjacency matrix for connectivity weight of ROIs pair i and j $\in \mathbb{R}^{n_r \times n_r}$
$\widehat{\mathbf{Y}}_i$	predicted graph view from the source graph view $\mathbf{X}_i$ for the i^{th} sujbect $\in \mathbb{R}^{n_r \times n_r}$
$\widehat{\mathbf{Y}}_i$	predicted graph view from the intermediate brain graph $\widehat{\mathbf{X}}_i$ for the i^{th} subject $\in \mathbb{R}^{n_r \times n_r}$
$\mathbf{U}$	random noise $\in \mathbb{R}^{n_r \times n_r}$
$s(\mathbf{i})$	topological strength of the ROI i
λ	constant value

2.1. Brain graph translation by the GT GAN

To begin with, we adapt the GT GAN architecture proposed in (Guo et al., 2018) to brain connectomes. GT GAN aims at translating a source graph to the target graph. For an input graph $\mathbf{X} = (V, E, W)$, where V is the set of N nodes, $E \subseteq V \times V$ is the set of egdes and a weighted adjacency matrix $\mathbf{W} \in \mathbb{R}^{n_r \times n_r}$ storing the set of weights for edges, where $e_{i,j} \in E$ links node $v_i \in V$ to $v_j \in V$. $\mathbf{W}_{i,j}$ is the weight assigned to the edge $e_{i,j}$. In our case, graph nodes are the anatomical brain ROIs, the weights for edges are connectivity weights between pairs of ROIs. For a subject i, we aim at translating a source brain graph view $\mathbf{X}_i$ to the target graph view $\mathbf{Y}_i$. GT GAN architecture is composed of a translator T and a graph discriminator D. Here, given an input graph $\mathbf{X}$, a translator T, trained to generate the target graph $\mathbf{Y}$, a graph discriminator D and random noise $\mathbf{U}$ which is introduced by dropout operation (Seltzer et al., 2013) in each convolution and deconvolution layers of the translator. T and D are adversarially trained to compete with other, where D acts as a binary classifier to distinguish between T's translated (i.e., predicted target from source) connectome $\widehat{\mathbf{Y}}$ and the target connectome $\mathbf{Y}$. The adverserial loss function $\mathcal{L}_{gan}$ for GT GAN's training process is expressed in the following **Eq.** 1:

$$\mathcal{L}_{gan}(T, D) = \mathbb{E}_{\mathbf{Y}}[\log(D(\mathbf{Y}))] + \mathbb{E}_{\mathbf{X},\mathbf{U}}[\log(1 - D(T(\mathbf{X}, \mathbf{U})))] \tag{1}$$

By considering findings in (Isola et al., 2017), where better results were attained by including $\mathcal{L}1$ loss on the GAN loss, the $\mathcal{L}1$ loss is computed on the weights of adjacency matrices of generated brain connectomes and ground truth target brain connectomes as shown below:

$$\begin{aligned} \mathcal{L}1(T, D) &= \mathbb{E}_{\mathbf{X},\mathbf{Y}}[\|\mathbf{Y} - \widehat{\mathbf{Y}}\|_1] \\ where\ \widehat{\mathbf{Y}} &= T(\mathbf{X}, \mathbf{U}) \end{aligned} \tag{2}$$

We add the $\mathcal{L}1$ on the total generator loss, and the total loss $\mathcal{L}$ therefore becomes:

$$\mathcal{L}(T, D) = \mathcal{L}_{gan} + \lambda \mathcal{L}1(T, D) \tag{3}$$

λ regulates the weight attached to the $\mathcal{L}1$ loss. The training process is modeled as a min-max optimization problem over the adversarial loss function as follows:

$$T^* = argmin_T max_D \mathcal{L}(T, D) \tag{4}$$

T aims at maximizing the loss objective against an adverserial D that aims at minimizing it.

2.1.1. Brain graph translator

The brain graph translator is composed of convolution and deconvolution layers as shown in **Fig.** 2. It aims at simultaneously learning the latent patterns of brain connectomes and their generic translation mappings from the input brain connectomic view to the target one. Precisely, it focuses on learning both the general global (connectome level) translation mappings and the local brain ROIs properties transformations. Since brain connectomic patterns vary for each brain network sample, sample-specific latent representations need to be learned by the translation model. In order to meet this need, a skip-net structure (Ronneberger et al., 2015) is deployed so as to pass over sample-specific connectomic representations to the decoder's layers via the skip connections. The sample invariant brain connectomic mappings are learnt in the encoder-decoder architecture. Brain network deconvolution, an extension of graph convolution is adopted in order to preserve global and local brain network information. The brain graph translator (T) architecture is illustrated in **Fig.** 2 where the input brain connectome first undergoes two edge-to-edge convolutions meant for encoding higher-order topological information and later embedded into node representation by a edge-to-node convolution operation. Graph deconvolution layers consist of one node-to-edge deconvolution operation and two edge-to-edge deconvolution operations. The graph deconvolution operation is a reverse process of graph convolution as it decodes the single node or edge information to its connected neighbouring nodes or edges.

2.2. Cycle graph translation (CGT) GAN

In order to guarantee a bidirectional translation while optimizing the similarity between the translated (i.e., generated) and target brain connectomes, we propose to extend the GT GAN architecture to a cycle graph translation (CGT) GAN whose architecture is shown in **Fig.** 2. To this aim, we design two translators T_1 and T_2 such that:

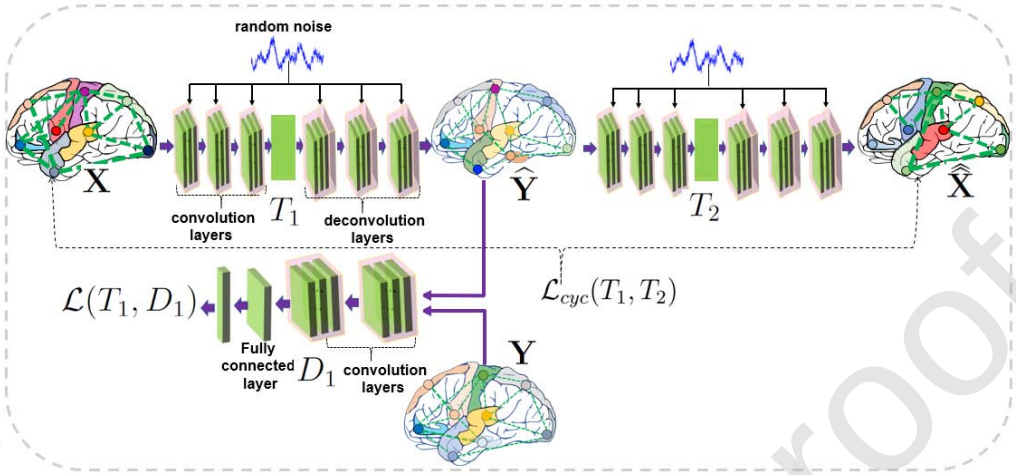

Figure 2: *Illustration of the proposed cyclic graph translation using topological strength (CGTS GAN) framework.* The CGTS GAN architecture is composed of two translator networks T_1 and T_2 with graph convolution and deconvolution layers. For the forward direction, $\mathbf{X}$ and $\mathbf{Y}$ are the source and target brain connectomic views respectively and in the reverse direction $\mathbf{Y}$ becomes the source view while $\mathbf{X}$ is the target one to predict. Translators T_1 and T_2 are trained adversarially with discriminators D_1 and D_2 respectively. D_2 is analogous to D_1 in the opposite direction. The framework allows bidirectional brain connectomic view translation between the source and target views with two learned mappings, T_1: $(\mathbf{X}, \mathbf{U}) \longrightarrow \widehat{\mathbf{Y}}$ and T_2: $(\mathbf{Y}, \mathbf{U}) \longrightarrow \widehat{\mathbf{X}}$, where $\mathbf{U}$ is a random noise. We enforce cycle consistency on the learning of both translators T_1 and T_2 with the cycle loss $\mathcal{L}_{cyc}(T_1, T_2)$ so that, if any source connectomic view is translated to the target one, and back again, we should be able to obtain the source view again. In the forward direction, $\widehat{\widehat{\mathbf{X}}} = T_2(\widehat{\mathbf{Y}}, \mathbf{U})$, and similarly in the opposite direction, $\widehat{\widehat{\mathbf{Y}}} = T_1(\widehat{\mathbf{X}}, \mathbf{U})$. We also integrate a graph topology-based loss where we aim to align the distribution of the predicted target graphs in node strength with that of the ground-truth ones.

$$\begin{cases} T_1 : (\mathbf{X}, \mathbf{U}) \longrightarrow \widehat{\mathbf{Y}} \\ T_2 : (\mathbf{Y}, \mathbf{U}) \longrightarrow \widehat{\mathbf{X}} \end{cases}$$

Similarly to the GT GAN, T_1 inputs the source brain connectomic graph $\mathbf{X}$ and the random noise $\mathbf{U}$, and outputs the predicted brain connectome $\widehat{\mathbf{Y}}$ for the target ground-truth connectome $\mathbf{Y}$. In a reversed manner, T_2 inputs the random noise and a source brain connectomic graph $\mathbf{Y}$ and outputs the reversely predicted source brain connectome $\widehat{\mathbf{X}}$ from the target ground-truth connectome. Translators T_1 and T_2 are adversarially trained with dis-

criminators D_1 and D_2 respectively, where D_1 is a binary classifier built on graph convolutional networks (GCN), distinguishing between generated connectome $\widehat{\mathbf{Y}}$ and the ground-truth connectome $\mathbf{Y}$, hence the adversarial training loss function $\mathcal{L}_{gan}$ is defined as follows:

$$\mathcal{L}_{gan}(T_1, D_1) = \mathbb{E}_{\mathbf{Y}}[\log(D_1(\mathbf{Y}))] + \mathbb{E}_{\mathbf{X},\mathbf{U}}[\log(1 - D_1(T_1(\mathbf{X}, \mathbf{U})))] \tag{5}$$

Next, we compute the $\mathcal{L}1$ loss as shown below:

$$\mathcal{L}1(T_1, D_1) = \mathbb{E}_{\mathbf{X},\mathbf{Y}}[\|\mathbf{Y} - \widehat{\mathbf{Y}}\|_1] \tag{6}$$

We then add the $\mathcal{L}1$ loss to the $\mathcal{L}_{gan}$ loss, hence the total loss becomes:

$$\mathcal{L}(T_1, D_1) = \mathcal{L}_{gan}(T_1, D_1) + \lambda\mathcal{L}1(T_1, D_1) \tag{7}$$

Likewise we define the loss of the second translator in our cyclic architecture as:

$$\mathcal{L}(T_2, D_2) = \mathcal{L}_{gan}(T_2, D_2) + \lambda\mathcal{L}1(T_2, D_2) \tag{8}$$

where λ regulates importance attached to the $\mathcal{L}1$ loss. To further enforce the similarity between the predicted and the target connectomes, we adopt the cycle consistency loss proposed in (Isola et al., 2017) where, for $\widehat{\widehat{\mathbf{X}}} = T_2(\widehat{\mathbf{Y}}, U)$, and $\widehat{\widehat{\mathbf{Y}}} = T_1(\widehat{\mathbf{X}}, U)$, we should be able to translate $\widehat{\widehat{\mathbf{X}}}$ back to the original brain graph $\mathbf{X}$ **Fig.** 2, likewise, $\widehat{\widehat{\mathbf{Y}}}$ should be translated back to its original brain graph $\mathbf{Y}$. These conditions are fulfilled by imposing cycle consistency loss on brain graph translators as shown below:

$$\mathcal{L}_{cyc}(T_1, T_2) = \mathbb{E}_X[\|\mathbf{X} - \widehat{\widehat{\mathbf{X}}}\|_1] + \mathbb{E}_{\mathbf{Y}}[\|\mathbf{Y} - \widehat{\widehat{\mathbf{Y}}}\|_1] \tag{9}$$

The total CGT GAN objective becomes:

$$\mathcal{L}(T_1, T_2, D_1, D_2) = \mathcal{L}(T_1, D_1) + \mathcal{L}(T_2, D_2) + \lambda_2\mathcal{L}_{cyc}(T_1, T_2) \tag{10}$$

where λ_2 is a hyperparameter to tune the cycle loss. By combining equations 7 and 8, we can achieve the bidirectional translation without necessarily imposing the cycle losses on the translators, and thus we term this as Bidirectional Graph Translation GAN (BGT GAN), whose total objective $\mathcal{L}_{bgt}$ is expressed as:

$$\mathcal{L}_{bgt}(T_1, T_2, D_1, D_2) = \mathcal{L}(T_1, D_1) + \mathcal{L}(T_2, D_2) \tag{11}$$

The bidirectional graph translation (BGT) GAN is trained in the same way as the CGT GAN but without the cycle losses.

2.3. Strength topological constraint

Given a graph with weights between its nodes embedded in an $n_r \times n_r$ weight matrix $\mathbf{W}$, the strength s of a node (brain ROI) i is the sum of the weights of all links attached to it:

$$s(i) = \sum_{j}^{n_r} \mathbf{W}_{ij} \tag{12}$$

where j represents all nodes (brain RIOs) other than i, n_r is the total number of nodes, and $\mathbf{W}_{ij}$ denotes the connectivity weight between nodes i and j, and is greater than 0 if node i is connected to node j. Our goal is to ensure that specifically, the strength topological properties of brain ROIs of the target connectomic view are well preserved in the generated views during the cyclic translation process. In order to achieve this, we impose the topological strength constraint on the learning of our GAN translators. The topological strength property is a natural measure of the node's importance or centrality in the network (Barrat et al., 2004). Physically, node strength is interpreted as a weight assigned to a node in a graph (Amano et al., 2018). For example, in world-wide international airport network, node strength quantifies the volume of traffic handled by each airport, while in financial networks it measures each individuals wealth. For a scientific collaboration network (Newman, 2001), it represents the number of articles published by each researcher and in human social life, it measures the total communication time spent by all individuals while communicating with each other in a certain time interval (Takaguchi et al., 2011). Brain ROI strength

is a weighted variant of the topological degree measure, which is commonly used for identifying hubs in brain networks (Fornito et al., 2016; Rubinov and Sporns, 2010). It differs from the degree measure in the sense that it accounts for link weights (Korhonen et al., 2017). Thus, node strength can capture both the topology information (existence of links) and the network weight distribution that serves a very vital role in uniquely characterizing nodes especially in fully connected and weighted networks like brain connectomes. Moreover, our approach can be easily extended to preserve other topological properties such as clustering coefficient. We propose to impose the strength constraint on GT, BGT, CGT GAN architectures, thereby producing new GTS, BGTS, CGTS architectures, where "S" signifies the inclusion of the topological strength constraint on any of these brain graph translation architectures. We achieve this by computing $\mathcal{L}1$ *loss* on the strength vectors of the predicted target and ground truth target graphs using the formula in **Eq.** 12. Next, we detail the total loss functions of the GTS, BGTS and CGTS $\mathcal{L}_{gts}$, $\mathcal{L}_{bgts}$ and $\mathcal{L}_{cgts}$, respectively.

2.3.1. Graph translation with strength topological constraint (GTS) GAN

We compute the $\mathcal{L}1$ *loss* on the strength vectors of the source and predicted brain graphs as $\mathcal{L}1_{stg}$ in the equation below:

$$\mathcal{L}1_{stg}(T_1, D_1) = \mathbb{E}_{\mathbf{X},\mathbf{Y}}[\|\mathbf{s}(\mathbf{Y}) - \mathbf{s}(\widehat{\mathbf{Y}})\|_1] \tag{13}$$

where $\mathbf{s}(\mathbf{X}) \in \mathbb{R}^{1\times n_r}$ is a vector storing the strength topological magnitude of each anatomical ROI in the the graph view $\mathbf{X}$.

The total objective loss $\mathcal{L}_{gts}(T, D)$ is then defined as:

$$\mathcal{L}_{gts}(T, D) = \mathcal{L}_{gan} + \lambda\mathcal{L}1(T, D) + \lambda_1 L1_{stg}(T_1, D_1) \tag{14}$$

λ and $\lambda 1$ are hyperparameters to tune the $\mathcal{L}1$ loss and the topological strength constraint respectively.

2.3.2. *Bidirectional graph translation with strength topological constraint (BGTS) GAN*

In a similar way, we define the new total BGTS loss $\mathcal{L}_{bgts}$ by adding the topology constraint as follows:

$$\begin{aligned}\mathcal{L}_{bgts}(T_1, T_2, D_1, D_2) =& \mathcal{L}(T_1, D_1) + \mathcal{L}(T_2, D_2) \\ &+ \lambda_1[\mathcal{L}1_{stg}(T_1, D_1) + \mathcal{L}1_{stg}(T_2, D_2)]\end{aligned} \tag{15}$$

where $\mathcal{L}1_{stg}(T_2, D_2)$ is analogous to $\mathcal{L}1_{stg}(T_1, D_1)$ for network pairs T_2 and D_2.

2.3.3. *Cyclic graph translation with strength topological constraint GAN (CGTS GAN)*

Here, we not only aim at having bidirectional brain view translation while ensuring that the strength topological patterns of the brain ROIs in the target view are preserved in the predicted view, but we also intend to achieve significant similarity between the translated and target views. Hence, we impose both cycle loss and the strength topological constraints on the translator learning as shown below:

$$\mathcal{L}_{cyc,stg}(T_1, T_2) = \mathbb{E}_{\mathbf{X}}[\|\mathbf{s}(\mathbf{X}) - \mathbf{s}(\widehat{\mathbf{X}})\|_1] + \mathbb{E}_{\mathbf{Y}}[\|\mathbf{s}(\mathbf{Y}) - \mathbf{s}(\widehat{\mathbf{Y}})\|_1] \tag{16}$$

The total objective function of the CGTS GAN, $\mathcal{L}_{cgts}$ is expressed as follows:

$$\begin{aligned}\mathcal{L}_{cgts}(T_1, T_2, D_1, D_2) =& \mathcal{L}(T_1, D_1) + \mathcal{L}(T_2, D_2) \\ &+ \lambda_1[\mathcal{L}1_{stg}(T_1, D_1) + \mathcal{L}1_{stg}(T_2, D_2)] \\ &+ \lambda_2\mathcal{L}_{cyc,stg}(T_1, T_2)\end{aligned} \tag{17}$$

$\lambda 1$ and $\lambda 2$ regulate the weights attached to the topological strength constraint and the cycle loss, respectively. Our CGTS-GAN code is available at https://github.com/basiralab/CGTS-GAN.

3. Results

Evaluation dataset. To evaluate our proposed framework, we used 150 subjects from the Autism Brain Imaging Data Exchange (ABIDE I) public

dataset [1]. For each subject, both right and left cortical hemispheres (RH and LH) were reconstructed using FreeSurfer (Fischl, 2012). Then, each cortical hemisphere was split into 35 cortical regions using Desikan-Killiany atlas (Desikan et al., 2006). Four cortical attributes were assigned to each vertex on the cortical surface using FreeSurfer. These attributes are the maximum principal curvature, the cortical thickness, the sulcal depth, and the average curvature. Based on these attributes, four morphological networks (also called views) were generated for each subject. For each cortical view, the weight of the connectivity between two ROIs i and j is computed as the absolute difference between the average cortical attribute in ROI i and the average cortical attribute in ROI j (Mahjoub et al., 2018; Lisowska et al., 2018; Dhifallah et al., 2019b). We used four views for LH and we named them view1, view2, view3 and view4, respectively. We illustrate both connectivity weight and topological strength distributions of the brain ROIs in the ground truth views and predicted views by the different translation GAN architectures by plotting their kernel density estimates (KDEs) (Silverman, 1986). KDEs are closely related to histograms but more superior in accuracy, and they allow continuity, there by making it easier to understand modality, symmetry, skewness and center of the distribution by looking at continuous lines. Moreover, accuracy of histograms is highly affected by parameters like bin sizes unlike KDEs where such parameters are not necessary.

Parameter setting. In all experiments, we heuristically set $\lambda = 10$, $\lambda 1 = 0.01$, $\lambda 2 = 0.01$, epochs to 200, discriminator learning rate to 0.0001, the generator learning rate to 0.00005, and we used ADAM optimizer (Kingma and Ba, 2014) for the optimization of the learning models.

Evaluation measures. We trained all the GAN architectures using 5-fold cross-validation (5-fold-CV). We randomly divided data samples into 5 folds, four folds were used for training and one left-out for testing in each cross-validation run. In the training phase, the model learns to translate from the source view to the target one. In the testing phase, the model is fed with test source brain connectome and outputs the predicted target connectome. We then compare the predicted connectomic view with the target one (ground

[1] http://preprocessed-connectomes-project.org/abide/

truth). We use the mean squared error (MSE) as evaluation metric:

$$MSE = \frac{1}{N}\sum_{i=1}^{N}(\mathbf{Y}_i - \widehat{\mathbf{Y}_i})^2 \tag{18}$$

where $\mathbf{Y}$ is the target view. $\widehat{\mathbf{Y}}$ denotes the predicted target view. N represents the number of subjects in the dataset. We translate each view to other views with different GAN translation architectures we have earlier discussed in Section 2, e.g., we translate view1 to views 2, 3, and 4. We report the MSE scores of each translation architecture during these translation by each architecture, namely GTS, BGTS, CGT, BGT, GTS, GT and GT-CD. We thereafter obtain the average MSE score of each particular translation architecture on a source view translation to other target views. Average MSE scores of translation architectures are shown in **Fig.** 3. In order to have an overall comparison of the performance of the proposed brain connectome generative architectures, we report the average MSE for all translations from all source views. **Fig.** 4 shows the overall average MSE scores for all translation architectures from all source views. Our proposed CGTS has the least MSE score, outperforming the baseline GT-CD and its ablated versions. In general, bidirectional-based translation architectures outperformed their unidirectional-based counterparts.

Comparison methods. In **Fig.** 4, we compare all the MSE scores of all proposed GAN architectures and the original graph translation GAN (Guo et al., 2018). As we gradually add architectural elements to the original graph translation GAN, we observe the target brain connectome prediction outcomes so as to evaluate the impact of each architectural component towards our desired goal. Firstly, we consider the original graph translation GAN architecture with its conditioned discriminator (GT-CD) GAN. We then consider an architecture built without conditioning the learning of the discriminator on the input graph (GT GAN). We thereafter gradually add other architectural components such as bidirectionality and target topology preservation to produce advanced versions of the GT GAN as described in **Section** 2.

In **Fig.** 5, we plot the brain ROIs connectivity weight distributions of the predicted views by the different brain graph translation GAN architectures in relation to the ground truth target connectivity weight distributions. Generally, translation models of different translation architectures are observed to have learnt the modalities of target data distributions effectively though

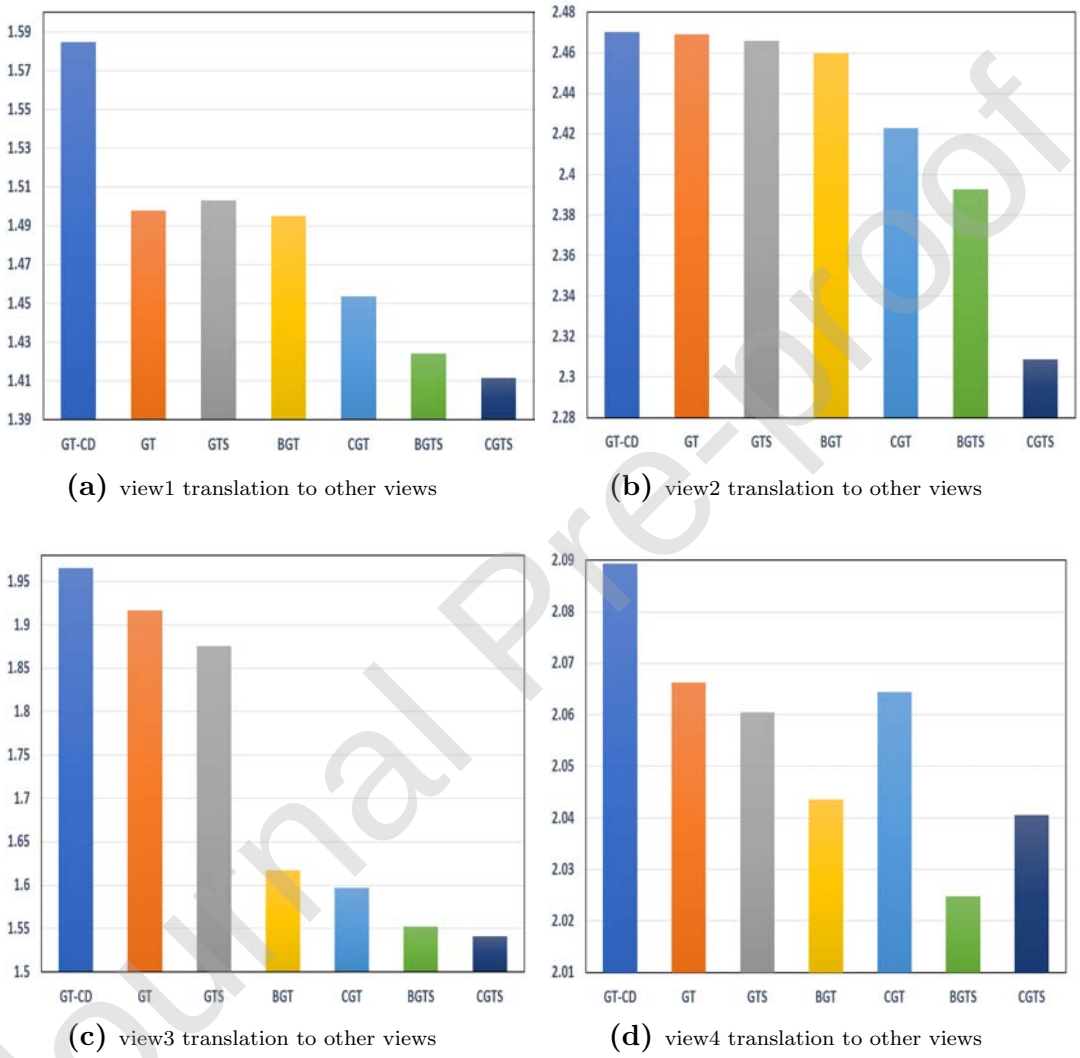

(a) view1 translation to other views

(b) view2 translation to other views

(c) view3 translation to other views

(d) view4 translation to other views

Figure 3: *Average MSE score for translation of views by the different translation GAN architectures*, the y-axis represents the average MSE and the x-axis shows the different translation GAN architectures.

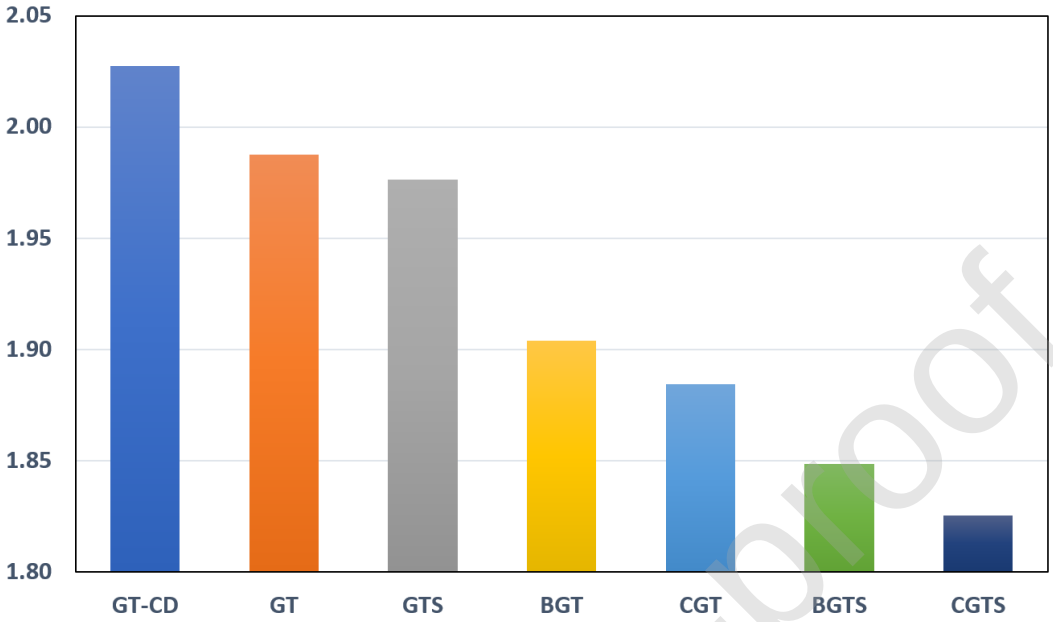

Figure 4: *Overall average MSE score for all views translations for the different translation GAN architectures*, the y-axis represents the average MSE and the x-axis shows the different translation GAN architectures.

with varying magnitudes of accuracies.

Brain ROIs topological strength distributions of predicted views for the different brain graph translation methods. Since one of our objectives is to predict brain connectomes where the topological strength distribution of the brain ROIs in the target view is aligned with that of the predicted view, in **Fig.** 6 we illustrate sample translations to compare the node strength distributions of connectomic views predicted by graph translation architectures with topological strength constraints (GTS, BGTS and CGTS) with the other architectures without the topological strength constraint (GT, BGT and CGT), in relation to the ground truth target topological strength distributions. Clearly, our proposed CGTS architecture exhibits better performance over original graph translation architecture and its ablated versions.

4. Discussion

In this paper, we proposed a cyclic brain connectome generation architecture with a strength topological constraint to (i) enforce a bidirectional brain connectomic view translation, (ii) maximize the similarity between the

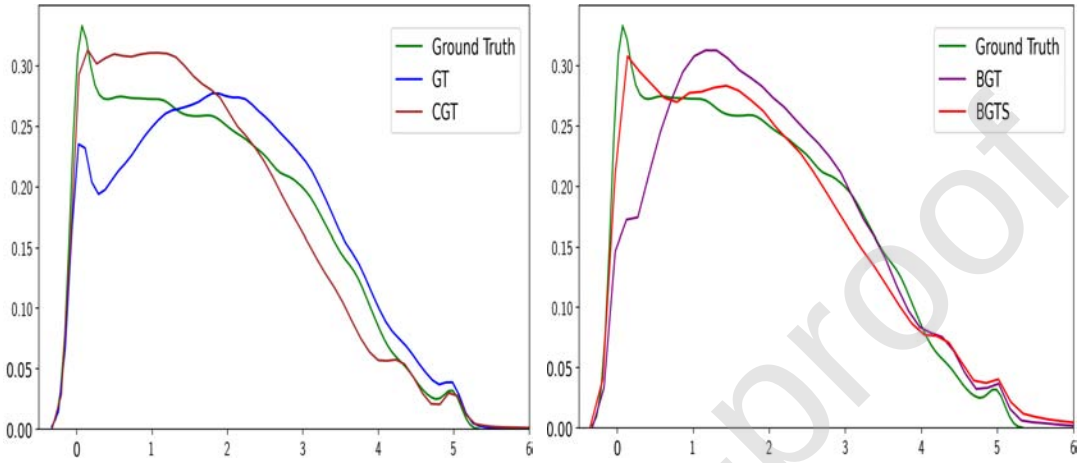

(a) view3 to view2 translation CGT vs. GT **(b)** view3 to view2 translation BGTS vs. BGT

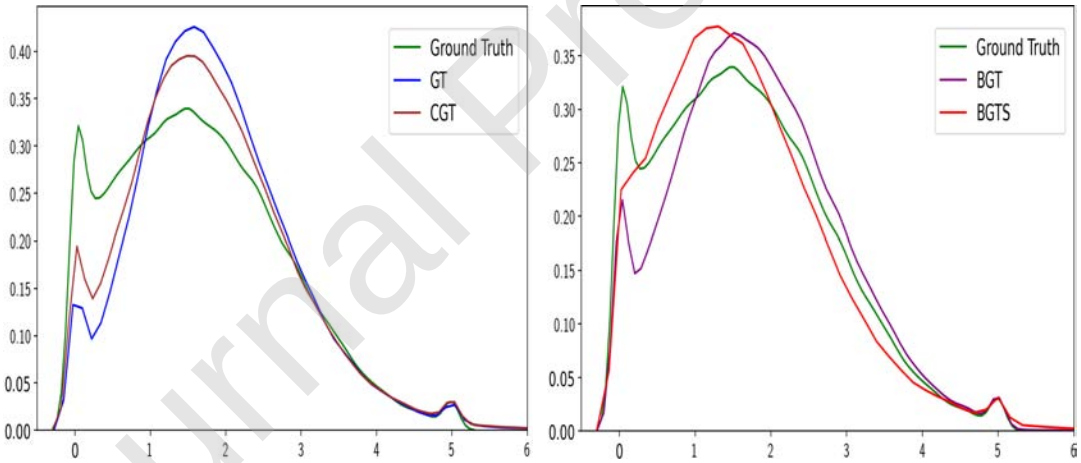

(c) view1 to view4 translation CGT vs. GT **(d)** view1 to view4 translation BGTS vs. BGT

Figure 5: *Analysis of brain ROIs connectivity weight distributions for predicted views by different GAN architectures.* Kernel density estimate for brain ROIs connectivity weight distributions for ground truth (target) view and predicted views by the different proposed translation GAN architectures for a few brain graph prediction tasks such as predicting view 2 from view3.

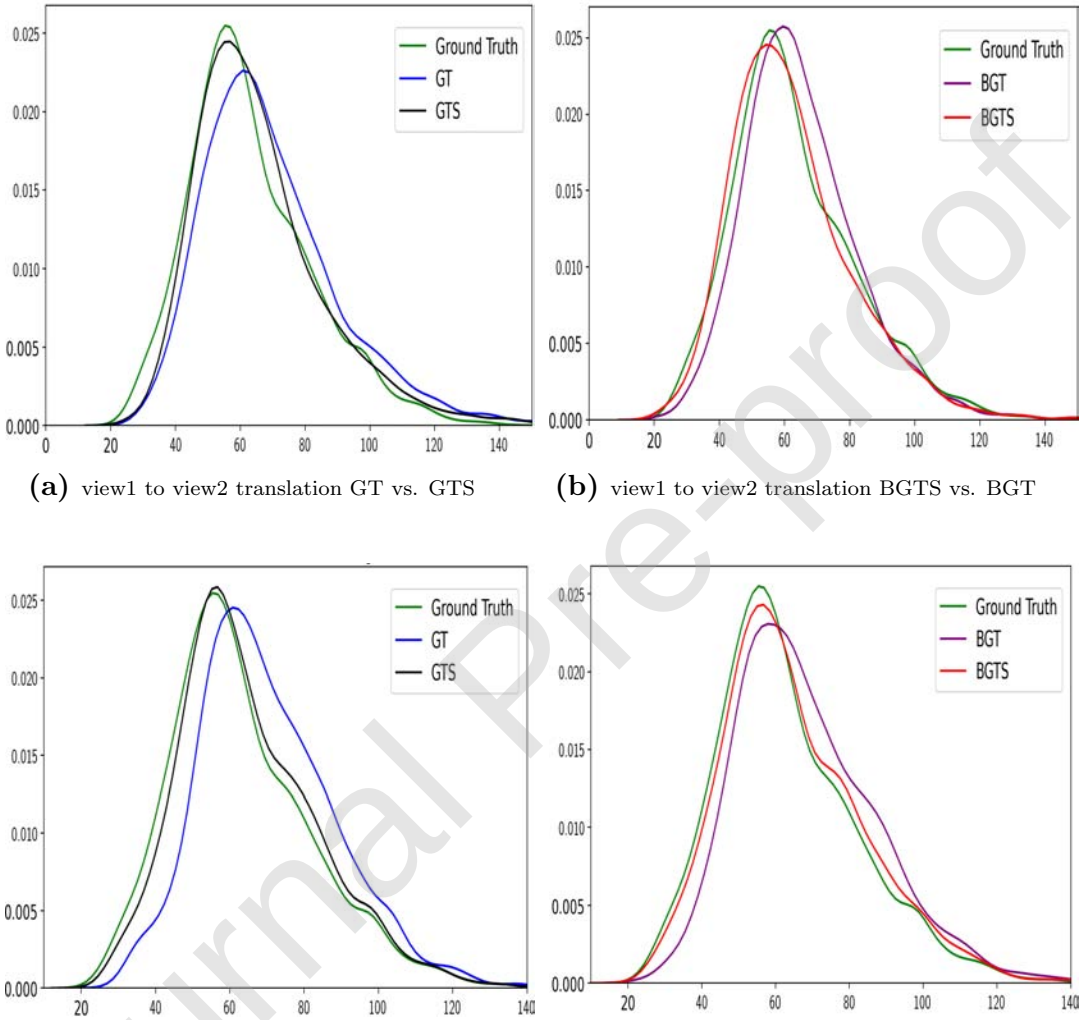

(a) view1 to view2 translation GT vs. GTS

(b) view1 to view2 translation BGTS vs. BGT

(c) view3 to view2 translation GTS vs. GT

(d) view3 to view2 translation BGTS vs. BGT

Figure 6: *Investigating the effect of the strength topological constraint.* Kernel density estimate for brain ROIs' topological strength distributions for the ground truth (target) view and views predicted by the different proposed GAN architectures in different prediction tasks. GTS vs. GT, BGTS vs. BGT, where in each case the former eg. GTS has a strength constraint "S", and the latter eg. GT is without the strength constraint. (a) and (b) illustrate view1 to view2 brain graph predictions while (c) and (d) for view3 to view2 predictions.

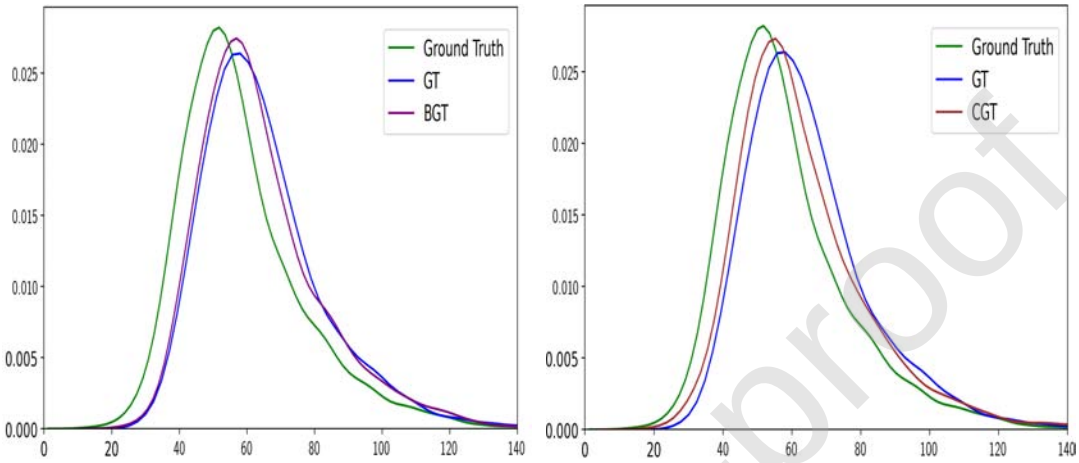

(a) view1 to view4 translation BGT vs. GT **(b)** view1 to view4 translation CGT vs. GT

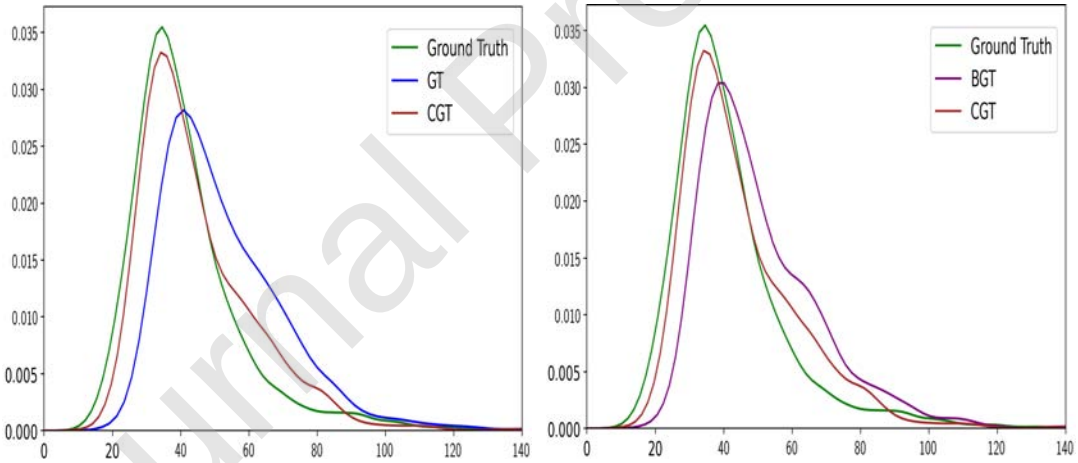

(c) view3 to view1 translation CGT vs. GT **(d)** view3 to view1 translation CGT vs. BGT

Figure 7: *Investigating the effect of the cycle loss.* Kernel density estimate for brain ROIs' strength distributions for the ground truth (target) brain graph and predicted brain graphs by the different proposed translation GAN architectures for selected prediction tasks. BGT vs. GT, CGT vs. GT in (a) and (b), respectively, and CGT vs. GT, CGT vs. BGT in (c) and (d), respectively.

predicted and target connectomic views, and (iii) ensure that the topological strength distribution of nodes in the target brain graphs is aligned with that of the predicted brain graphs. We achieved these objectives by imposing both the cycle loss and the strength topological constraints on the learning of the brain graph translators.

Analysis of prediction accuracy measurement with MSE. Enforcing a cycle consistency loss in CGT GAN architecture served the intended purpose of maximizing the similarity between the ground truth and the predicted graphs, and for this reason, CGTS GAN has the least average MSE in **Fig.** 4. The two-way directional translation in the bidirectional models including BGT and CGT yielded better performance as compared to unidirectional ones including GT, since our bidirectional models learnt extra data modal distributions mappings in the second direction translation. Bidirectional models like BGT, with no cycle loss constraints, allow more diversity in the predicted brain connectomes as compared to the cycle loss based models like CGT; thus, CGT has lower average MSE than BGT and so does for CGTS when compared to BGTS. By comparing the performance of GT GAN (with unconditioned discriminator) against that of GT-CD GANs in **Fig** 4, we notice that for our datasets, on average, it was generally not so significant to condition the learning of the discriminator on the input brain graph. Conditioned GANs (cGANs) are typically superior on predicting multi-modal distributions (Yang et al., 2019), which is not the case with our datasets (graph views) in general. In addition, as highlighted in (Pang and Liu, 2020) cGANs need relatively large training datasets to yield good results, yet we train on only 150 samples. Hence, for the rest of the translation GAN architectures, we relaxed the conditioning of the discriminator learning on the input brain network.

Bidirectional based translation (BGT and CGT) vs. unidirectional (GT) translation. Comparisons between bidirectional (BGT, CGT) and unidirectional (GT) based translations are shown in **Fig.** 7-(a,b), distribution of bidirectional translations based translations were closer to the target distributions (ground truth) than the undirectional ones. In bidirectional translations, during training, the model learnt extra information for matching distributions patterns of the source to target distributions due to the back and forth directional nature of the translation, hence outcompeting the unidirectional based translations.

Analysis of the strength constraint effect. In **Fig.** 6, we compared cases with and without the strength topological constraint (i.e., GTS vs. GT,

BGTS vs. BGT) . The distribution patterns for translations with the topological strength constraint were generally closer to the ground truth topological strength distribution than the ones without the strength constraints. For example, in **Fig.** 6-(a), GTS was closer to the target distribution than GT. This demonstrates the importance of the topological strength constraint in guiding the learning of the brain translation model towards the conservation of the strength topological property of brain ROIs of the ground-truth target views in the predicted views.

Analyzing the cycle loss (CGT vs. GT) effect. In **Fig.** 7-(c,d), we investigated the effect of imposing the cycle loss constraint on the translators in the graph translation architectures by comparing CGT (graph translation architecture with cycle losses) and GT (similar graph translation architecture but without cycle losses). Clearly, CGT-based distributions were closer to the target distribution and depicted the target graph distribution profile better than GT and BGT-based distributions since the cycle loss constraint enhanced the similarity between the target and predicted domains (Zhou et al., 2019).

Analyzing connectivity weight distributions of predicted views of by different architectures in relation to the target distributions. In **Fig.** 5-(a,c), we observe that the CGT GAN based distributions were closer to the target distributions than GT GAN, since the CGT GAN utilized the advantage of the cycle constraint and bidirectional translation as explained in the above analysis. Furthermore, in **Fig.** 5-(b,d), BGTS-based distributions were closer to the target distributions in comparison with BGT GAN-based distributions thanks to the strength topological constraint in the BGTS GAN. Generally, by imposing the strength topological constraint on the brain graph translators we not only achieved the goal of preserving the topological strength distribution of the source brain views in the translated views but we also improved the accuracy of predicted views as their brain ROIs connectivity weight distributions got closer to the target connectivity weight distributions.

Limitations and future work. Our work has some limitations. First, we heuristically set the parameters for regulating the weight of the strength constraint, implying that our parameter values were not necessarily optimal, learning how to automatically tune these parameters could yield better results. Second, our work is limited to a two-way directional translation. In the future work, to fasten the translation, we will adopt a multi-directional brain connectomic view translation approach inspired by the works in (Yu

et al., 2020; Chen and Denoyer, 2017) to train a translation model that simultaneously learns to predict in multiple (more than two) directions.

5. Conclusion

In this paper, we proposed a novel cycle-based and topology-aware brain graph prediction framework from a source graph. We adopted a cycle consistency architecture to enforce bidirectional translation between the source and target graphs. We also ensured that the essential strength topological property of the brain ROIs in the target view is significantly aligned with that of the target view by imposing the strength constraint on the learning of translators, which not only pushes the topological strength distribution of the predicted brain connectomic views to near that of the target ground-truth view, but also shifts the entire ROIs connectivity weight distribution of the predicted view closer to the connectivity weight distributions of the target view. We have shown the role and effect of each architectural component of the translation architectures we proposed in relation to our overall objective. So far, we focused on aligning the topology strength distribution of the ground-truth target graphs and that of the predicted graphs. Notably, our framework can easily be extended to conserving more topological properties such as eigenvector and betweenness centralities on not only brain connectomes but also other datasets including transport networks and epidemiological networks for disease outbreak detection.

6. Acknowledgements

This project has been funded by the 2232 International Fellowship for Outstanding Researchers Program of TUBITAK (Project No:118C288) supporting I. Rekik. However, all scientific contributions made in this project are owned and approved solely by the authors.

Declarations of interest: none to disclose.

Amano, S.i., Ogawa, K.i., Miyake, Y., 2018. Node property of weighted networks considering connectability to nodes within two degrees of separation. Scientific reports 8, 1–8.

Armanious, K., Jiang, C., Fischer, M., Küstner, T., Hepp, T., Nikolaou, K., Gatidis, S., Yang, B., 2020. Medgan: Medical image translation using gans. Computerized Medical Imaging and Graphics 79, 101684.

Barrat, A., Barthelemy, M., Pastor-Satorras, R., Vespignani, A., 2004. The architecture of complex weighted networks. Proceedings of the national academy of sciences 101, 3747–3752.

Bassett, D.S., Sporns, O., 2017. Network neuroscience. Nature neuroscience 20, 353–364.

Bessadok, A., Mahjoub, M.A., Rekik, I., 2019a. Hierarchical adversarial connectomic domain alignment for target brain graph prediction and classification from a source graph, in: International Workshop on PRedictive Intelligence In MEdicine, Springer. pp. 105–114.

Bessadok, A., Mahjoub, M.A., Rekik, I., 2019b. Symmetric dual adversarial connectomic domain alignment for predicting isomorphic brain graph from a baseline graph, in: International Conference on Medical Image Computing and Computer-Assisted Intervention, Springer. pp. 465–474.

Bronstein, M.M., Bruna, J., LeCun, Y., Szlam, A., Vandergheynst, P., 2017. Geometric deep learning: going beyond euclidean data. IEEE Signal Processing Magazine 34, 18–42.

Bullmore, E., Sporns, O., 2009. Complex brain networks: graph theoretical analysis of structural and functional systems. Nature reviews neuroscience 10, 186–198.

Bullmore, E.T., Bassett, D.S., 2011. Brain graphs: graphical models of the human brain connectome. Annual review of clinical psychology 7, 113–140.

Chen, M., Denoyer, L., 2017. Multi-view generative adversarial networks, in: Joint European Conference on Machine Learning and Knowledge Discovery in Databases, Springer. pp. 175–188.

Damoiseaux, J.S., Rombouts, S., Barkhof, F., Scheltens, P., Stam, C.J., Smith, S.M., Beckmann, C.F., 2006. Consistent resting-state networks across healthy subjects. Proceedings of the national academy of sciences 103, 13848–13853.

delEtoile, J., Adeli, H., 2017. Graph theory and brain connectivity in alzheimers disease. The Neuroscientist 23, 616–626.

Desikan, R.S., Ségonne, F., Fischl, B., Quinn, B.T., Dickerson, B.C., Blacker, D., Buckner, R.L., Dale, A.M., Maguire, R.P., Hyman, B.T., et al., 2006. An automated labeling system for subdividing the human cerebral cortex on mri scans into gyral based regions of interest. Neuroimage 31, 968–980.

Dhifallah, S., Rekik, I., Initiative, A.D.N., et al., 2019a. Clustering-based multi-view network fusion for estimating brain network atlases of healthy and disordered populations. Journal of neuroscience methods 311, 426–435.

Dhifallah, S., Rekik, I., Initiative, A.D.N., et al., 2019b. Clustering-based multi-view network fusion for estimating brain network atlases of healthy and disordered populations. Journal of neuroscience methods 311, 426–435.

Dhifallah, S., Rekik, I., Initiative, A.D.N., et al., 2020. Estimation of connectional brain templates using selective multi-view network normalization. Medical Image Analysis 59, 101567.

Farrell, C., Chappell, F., Armitage, P., Keston, P., MacLullich, A., Shenkin, S., Wardlaw, J., 2009. Development and initial testing of normal reference mr images for the brain at ages 65–70 and 75–80 years. European radiology 19, 177–183.

Fischl, B., 2012. Freesurfer. Neuroimage 62, 774–781.

Fornito, A., Zalesky, A., Bullmore, E., 2016. Fundamentals of brain network analysis. Academic Press.

Goodfellow, I., 2016. Nips 2016 tutorial: Generative adversarial networks. arXiv preprint arXiv:1701.00160 .

Guo, X., Wu, L., Zhao, L., 2018. Deep graph translation. arXiv preprint arXiv:1805.09980 .

Hinrichs, C., Singh, V., Xu, G., Johnson, S.C., Initiative, A.D.N., et al., 2011. Predictive markers for ad in a multi-modality framework: an analysis of mci progression in the adni population. Neuroimage 55, 574–589.

Huang, L., Jin, Y., Gao, Y., Thung, K.H., Shen, D., Initiative, A.D.N., et al., 2016. Longitudinal clinical score prediction in alzheimer's disease with soft-split sparse regression based random forest. Neurobiology of aging 46, 180–191.

Isola, P., Zhu, J.Y., Zhou, T., Efros, A.A., 2017. Image-to-image translation with conditional adversarial networks, in: Proceedings of the IEEE conference on computer vision and pattern recognition, pp. 1125–1134.

Jeste, S.S., Frohlich, J., Loo, S.K., 2015. Electrophysiological biomarkers of diagnosis and outcome in neurodevelopmental disorders. Current opinion in neurology 28, 110–116.

Kazeminia, S., Baur, C., Kuijper, A., van Ginneken, B., Navab, N., Albarqouni, S., Mukhopadhyay, A., 2018. Gans for medical image analysis. arXiv preprint arXiv:1809.06222 .

Kingma, D.P., Ba, J., 2014. Adam: A method for stochastic optimization. arXiv preprint arXiv:1412.6980 .

Kipf, T.N., Welling, M., 2016. Semi-supervised classification with graph convolutional networks. arXiv preprint arXiv:1609.02907 .

Korhonen, O., Saarimäki, H., Glerean, E., Sams, M., Saramäki, J., 2017. Consistency of regions of interest as nodes of fmri functional brain networks. Network Neuroscience 1, 254–274.

Levie, R., Monti, F., Bresson, X., Bronstein, M.M., 2018. Cayleynets: Graph convolutional neural networks with complex rational spectral filters. IEEE Transactions on Signal Processing 67, 97–109.

Li, Y., Vinyals, O., Dyer, C., Pascanu, R., Battaglia, P., 2018. Learning deep generative models of graphs. arXiv preprint arXiv:1803.03324 .

Lisowska, A., Rekik, I., disease neuroimaging initiative (ADNI), T.A., 2018. Joint pairing and structured mapping of convolutional brain morphological multiplexes for early dementia diagnosis. Brain connectivity 9, 22–36.

Lisowska, A., Rekik, I., Initiative, A.D.N., et al., 2017. Pairing-based ensemble classifier learning using convolutional brain multiplexes and multi-view brain networks for early dementia diagnosis.

Mahapatra, D., Bozorgtabar, B., Hewavitharanage, S., Garnavi, R., 2017. Image super resolution using generative adversarial networks and local saliency maps for retinal image analysis, in: International Conference on Medical Image Computing and Computer-Assisted Intervention, Springer. pp. 382–390.

Mahjoub, I., Mahjoub, M.A., Rekik, I., 2018. Brain multiplexes reveal morphological connectional biomarkers fingerprinting late brain dementia states. Scientific reports 8, 4103.

Pan, S., Hu, R., Long, G., Jiang, J., Yao, L., Zhang, C., 2018. Adversarially regularized graph autoencoder for graph embedding. arXiv preprint arXiv:1802.04407 .

Pang, Y., Liu, Y., 2020. Conditional generative adversarial networks (cgan) for aircraft trajectory prediction considering weather effects, in: AIAA Scitech 2020 Forum, p. 1853.

Raeper, R., Lisowska, A., Rekik, I., 2018. Cooperative correlational and discriminative ensemble classifier learning for early dementia diagnosis using morphological brain multiplexes. IEEE Access 6, 43830–43839.

Reijneveld, J.C., Ponten, S.C., Berendse, H.W., Stam, C.J., 2007. The application of graph theoretical analysis to complex networks in the brain. Clinical neurophysiology 118, 2317–2331.

Ronneberger, O., Fischer, P., Brox, T., 2015. U-net: Convolutional networks for biomedical image segmentation, in: International Conference on Medical image computing and computer-assisted intervention, Springer. pp. 234–241.

Rubinov, M., Sporns, O., 2010. Complex network measures of brain connectivity: uses and interpretations. Neuroimage 52, 1059–1069.

Samanta, B., Abir, D., Jana, G., Chattaraj, P.K., Ganguly, N., Rodriguez, M.G., 2019. Nevae: A deep generative model for molecular graphs, in:

Proceedings of the AAAI Conference on Artificial Intelligence, pp. 1110–1117.

Seltzer, M.L., Yu, D., Wang, Y., 2013. An investigation of deep neural networks for noise robust speech recognition, in: 2013 IEEE international conference on acoustics, speech and signal processing, IEEE. pp. 7398–7402.

Silverman, B.W., 1986. Density estimation for statistics and data analysis. volume 26. CRC press.

Simonovsky, M., Komodakis, N., 2018. Graphvae: Towards generation of small graphs using variational autoencoders, in: International Conference on Artificial Neural Networks, Springer. pp. 412–422.

Soares, J.M., Magalhães, R., Moreira, P.S., Sousa, A., Ganz, E., Sampaio, A., Alves, V., Marques, P., Sousa, N., 2016. A hitchhiker's guide to functional magnetic resonance imaging. Frontiers in neuroscience 10, 515.

Takaguchi, T., Nakamura, M., Sato, N., Yano, K., Masuda, N., 2011. Predictability of conversation partners. Physical Review X 1, 011008.

Tong, T., Gray, K., Gao, Q., Chen, L., Rueckert, D., 2015. Nonlinear graph fusion for multi-modal classification of alzheimers disease, in: International Workshop on Machine Learning in Medical Imaging, Springer. pp. 77–84.

de Vico Fallani, F., Richiardi, J., Chavez, M., Achard, S., 2014. Graph analysis of functional brain networks: practical issues in translational neuroscience. Philosophical Transactions of the Royal Society B: Biological Sciences 369, 20130521.

Wang, Y., Ma, G., An, L., Shi, F., Zhang, P., Lalush, D.S., Wu, X., Pu, Y., Zhou, J., Shen, D., 2016. Semisupervised tripled dictionary learning for standard-dose pet image prediction using low-dose pet and multimodal mri. IEEE Transactions on Biomedical Engineering 64, 569–579.

Wu, E., Wu, K., Cox, D., Lotter, W., 2018. Conditional infilling gans for data augmentation in mammogram classification, in: Image Analysis for Moving Organ, Breast, and Thoracic Images. Springer, pp. 98–106.

Wu, Z., Pan, S., Chen, F., Long, G., Zhang, C., Philip, S.Y., 2020. A comprehensive survey on graph neural networks. IEEE Transactions on Neural Networks and Learning Systems .

Yang, D., Hong, S., Jang, Y., Zhao, T., Lee, H., 2019. Diversity-sensitive conditional generative adversarial networks. arXiv preprint arXiv:1901.09024 .

Yi, X., Walia, E., Babyn, P., 2019. Generative adversarial network in medical imaging: A review. Medical image analysis , 101552.

You, J., Ying, R., Ren, X., Hamilton, W.L., Leskovec, J., 2018. Graphrnn: Generating realistic graphs with deep auto-regressive models. arXiv preprint arXiv:1802.08773 .

Yu, W., Chang, T., Guo, X., Wang, X., Liu, B., He, Y., 2020. Ugan: Unified generative adversarial networks for multidirectional text style transfer. IEEE Access 8, 55170–55180.

Yuan, L., Wang, Y., Thompson, P.M., Narayan, V.A., Ye, J., Initiative, A.D.N., et al., 2012. Multi-source feature learning for joint analysis of incomplete multiple heterogeneous neuroimaging data. NeuroImage 61, 622–632.

Zhang, D., Wang, Y., Zhou, L., Yuan, H., Shen, D., Initiative, A.D.N., et al., 2011. Multimodal classification of alzheimer's disease and mild cognitive impairment. Neuroimage 55, 856–867.

Zhou, D., Zheng, L., Xu, J., He, J., 2019. Misc-gan: A multi-scale generative model forgraphs. Frontiers in Big Data 2, 3.

Zhou, J., Cui, G., Zhang, Z., Yang, C., Liu, Z., Wang, L., Li, C., Sun, M., 2018. Graph neural networks: A review of methods and applications. arXiv preprint arXiv:1812.08434 .

Zhu, J.Y., Park, T., Isola, P., Efros, A.A., 2017. Unpaired image-to-image translation using cycle-consistent adversarial networks, in: Proceedings of the IEEE international conference on computer vision, pp. 2223–2232.

Zhu, M., Rekik, I., 2018. Multi-view brain network prediction from a source view using sample selection via cca-based multi-kernel connectomic manifold learning, in: International Workshop on PRedictive Intelligence In MEdicine, Springer. pp. 94–102.

* We propose a topology-constrained prediction of brain connectomes.
* We design a graph GAN for predicting a target brain graph from a source one.
* Our CGTS GAN propels the field of predictive network neuroscience.

Journal of Neuroscience Methods

TOPOLOGY-GUIDED CYCLIC BRAIN CONNECTIVITY GENERATION USING GEOMETRIC DEEP LEARNING

Dr Islem Rekik
Director of Brain And SIgnal Research & Analysis (BASIRA) lab
Istanbul Technical University
Faculty of Computer and Informatics Engineering
tel: +90 212 2856782
email: irekik@itu.edu.tr
www.basira-lab.com
July 14, 2020

Credit author statement

Abubakhari Sserwadda: Methodology, Software, Formal analysis, Validation, Visualization, Writing- Original draft

Islem Rekik: Conceptualization, Supervision, Methodology, Resources, Writing- Reviewing and Editing, Funding acquisition

Kindly,
Islem Rekik on behalf of co-authors